LOCK EXCHANGE GRAVITY CURRENTS ON UPSLOPING BEDS

Claudia Adduce[1], Marco Leone[1], Valentina Lombardi[1], Giampiero Sciortino[1], Michele La Rocca[1] & Mario Morganti[1]

[1]Department of Civil Engineering, University of Rome "Roma Tre", Italy, Via Vito Volterra 62, 00146, Rome
E-mail: vlombardi@uniroma3.it; adduce@uniroma3.it

Abstract

This work deals with gravity currents moving on upsloping beds investigated by both experimental and numerical simulations. Laboratory experiments were realized by the lock exchange release technique in a Perspex tank of rectangular cross section, divided into two reservoirs by a vertical removable gate, one filled with colored salty water and the other one filled with clear fresh water with a lower density. When the gate is removed, the dense fluid collapses developing a gravity current under the surrounding fluid. Different values of the bed's slope were tested. Each experiment was recorded by a CCD camera and an image analysis technique, based on the threshold method, was applied to measure the space-time evolution of the current's profile and the time history of the front's position. Numerical simulations were carried out using a two-layer shallow water model, which accounts for both the free surface and the mixing between the two fluids. Two different relations are used to model the entrainment: the formula suggested by Adduce et al. (2012) and the formula of Cenedese & Adduce (2010). A comparison between numerical and experimental results was performed. Numerical simulations performed with Adduce et al. (2012) formula show a better agreement with the experimental results, if compared with the simulations using Cenedese and Adduce (2010) relation. In addition numerical simulations show, near the lock, an area in which the gravity current's velocity is negative, i.e. the dense fluid is moving downslope.

Introduction

Gravity currents are caused by a density gradient between two fluids and occur both in natural and in industrial flows. The driving force can be due to a dissolved solute (i.e. salt in the sea), to a difference of temperature, or to the presence of suspended sediments. Examples of gravity currents are given by avalanches, turbidity currents, pyroclastic flows, lava flows, sea-breeze and salt wedge propagation (Simpson, 1997).

Gravity currents were investigated by both laboratory experiments and numerical simulations. Models based on the shallow-water theory (Rottmann & Simpson, 1983; Shin et al., 2004; La Rocca et al., 2008; Adduce et al., 2012) were often used to simulate gravity currents. Rottmann & Simpson (1983) studied gravity currents by laboratory experiments and compared measurements with numerical solutions of the shallow water equations for a two-layer fluid bounded at top and bottom by rigid horizontal planes and at one end by a vertical wall, neglecting mixing effects between the two fluids. Benjamin (1968) developed a theory for the propagation of a steadily advancing current and focused the attention on the importance of dissipation in gravity current dynamics. Shin et al. (2004) provided a theory based on the energy-conserving flow that is in agreement with their experiments, and showed that dissipation is not important at high Reynolds numbers. La Rocca et al. (2008) studied the dynamics of 3D gravity currents on smooth and rough beds by lock exchange experiments and numerical simulations, performed by a shallow water model with immiscible liquids. Adduce et al. (2012) performed lock exchange experiments on a flat bed and compared experimental results with numerical simulations obtained by a two-layer, shallow water model accounting for both the free surface and entrainment. Turner (1986) entrainment relation, was modified by Adduce et al. (2012) in order to activate the mixing for the simulated gravity currents.

The aim of this paper is the investigation of gravity currents moving on upsloping beds by both laboratory experiments and numerical simulations. Four different bed's slopes were investigated by laboratory experiments and two different entrainment relations were tested in the numerical simulations.

Experimental apparatus

The experiments were conducted at the Hydraulics Laboratory of the University of Rome "Roma Tre", in a Perspex tank of rectangular cross-section, 3.0 m long, 0.3 m deep and 0.2 wide. The tank was divided in two parts by a vertical sliding gate placed at the distance x_0 from the left end wall of the tank, as shown in Figure 1. The left part of the tank was filled with salty water with an initial density ρ_{01}, while the right part was filled with tap water with

density ρ_2 and $\rho_{01}>\rho_2$. The depth of the two fluids at the gate was h_0. The experiment starts when the gate is removed, the salty water flows under the lighter fluid and the gravity current develops. The experiment stops when the gravity current reaches the right end wall of the tank. Such experimental technique is called "lock exchange release". Density measurements were performed by a pycnometer and a small quantity of dye was dissolved into the salty water to allow the visualization of the gravity current during the experiments.

Each experiment was recorded by a CCD camera, with a frequency of 25 Hz, and an image analysis technique, based on a threshold method, was applied to measure the space-time evolution of the gravity current's profile. The conversion factor pixel/cm was obtained using a rule placed along both the horizontal and vertical walls of the channel.

Four experiments were performed keeping constant $\rho_{01}\cong$1060 kg/m^3, ρ_2=1000 kg/m^3, h_0=0.15 m, x_0=0.1 m and by varying the angle θ between the bed and the horizontal, as it is shown in Table 1, where negative values of θ are referred to upsloping beds. The values of θ investigated were: +0.00°, -1.14°, -1.39° and -1.52°. θ=-1.39° is the "critical angle" for $\rho_{01}\cong$1060 kg/m^3 (Run 3), i.e. the angle for which the gravity current reaches the right end wall of the tank with a front's speed close to zero. The subcritical angle is defined as the angle for which the gravity current reaches the right end wall with a front's speed higher than zero (as in Run 2), while the supercritical angle is defined as the angle for which the current doesn't reach at all the right end wall of the tank (as in Run 4).

Table 1: Experimental parameters

RUN	ρ_{01}[kg/m^3]	θ [°]	*Angle*
1	1059.56	+0.00	0
2	1059.72	-1.14	subcritical
3	1059.75	-1.39	critical
4	1059.72	-1.52	supercritical

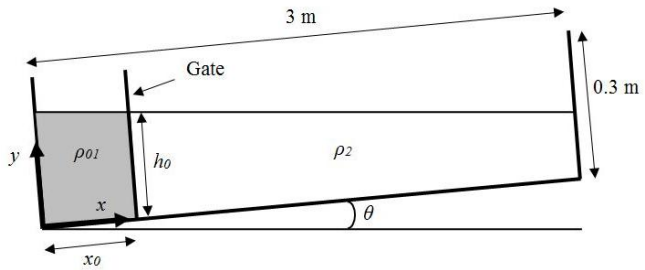

Figure 1: Sketch of the tank used to perform lock release gravity currents.

Mathematical model

A two-layer, 1D, shallow-water model was used to simulate gravity currents. Gravity currents frequently develop along the longitudinal direction, so that the ratio between the depth and the length of the current is small enough to allow the application of the shallow water theory. Previous papers investigating gravity currents by shallow water equations (Rottman & Simspon, 1983; Sparks et al., 1993; Hogg et al., 1999) assumed a steady free surface, while in the present work this hypothesis has been removed in order to have a more realistic solution, by modeling the space-time evolution of the free surface.

The mathematical model takes also into account the mixing between the two fluids. The entrainment at the interface, due to a mass transport from the lighter fluid to the heavier one, causes a decrease of the density of the gravity current. The entrainment between the two fluids was modeled by both a modified Turner's formula (1986), as in Adduce et al. (2012), and Cenedese & Adduce (2010) formula. Figure 2 shows the frame of reference used in the model.

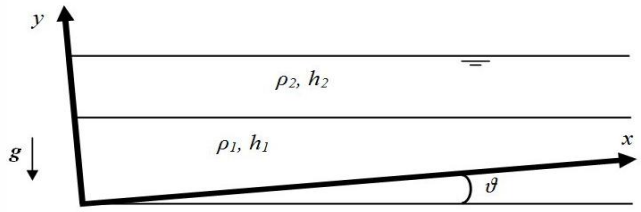

Figure 2: Frame of reference used in the mathematical model.

A 1D gravity current moving on a bed with a sloping angle θ is considered. For the mathematical model, negative values of θ are referred to upsloping beds. The heavier current of height h_1 and density ρ_1 flows below the lighter one of height h_2 and density ρ_2. Applying the principle of mass conservation and projecting along the x-axis the momentum equations, the following hyperbolic system of four partial differential equations is obtained:

$$\begin{cases} \dfrac{\partial(\rho_1 h_1)}{\partial t} h_1 + \dfrac{\partial(\rho_1 V_1 h_1)}{\partial x} = \rho_2 V_E \\ \dfrac{\partial(\rho_2 h_2)}{\partial t} + \dfrac{\partial(\rho_2 V_2 h_2)}{\partial x} = -\rho_2 V_E \\ \dfrac{\partial V_1}{\partial t} = g\sin\theta - \dfrac{\partial}{\partial x}\left[g\cos\theta \dfrac{\rho_1 h_1 + \rho_2 h_2}{\rho_1} + \dfrac{V_1^2}{2} \right] - \dfrac{\tau_{1b} - \tau_{12}}{\rho_1 h_1} \\ \dfrac{\partial V_2}{\partial t} = g\sin\theta - \dfrac{\partial}{\partial x}\left[(h_1 + h_2) g\cos\theta + \dfrac{V_2^2}{2} \right] - \dfrac{\tau_{12} + \tau_{2b}}{\rho_2 h_2} \end{cases} \quad (1)$$

where the unknown quantities h_1, h_2, V_1 and V_2 are the depth and the velocity of the lower and the upper layer, respectively. V_e is the entrainment velocity, τ_{1b} is the shear stress caused by the bottom and side walls for the lower layer, τ_{2b} is the shear stress caused by the side walls for the upper layer and τ_{12} is the shear stress at the interface between the two fluids. τ_{1b} and τ_{2b} are modeled by Darcy-

Weisbach's formula as in La Rocca et al. (2008) and Adduce et al. (2012):

$$\begin{cases} \tau_{1f} = \lambda_1 \rho_1 \dfrac{V_1|V_1|}{8} \dfrac{2h_1 + B}{B} \\ \tau_{2f} = \lambda_2 \rho_2 \dfrac{V_2|V_2|}{8} \dfrac{2h_2}{B} \end{cases} \quad (2)$$

where B is the width of tank; λ_1 and λ_2 are the friction factors for the lower and upper layer, respectively. The definition of λ_i, i.e. the friction factor for the i^{th} layer, was given by Colebrook (1939) for the transition between laminar and turbulent flow:

$$\lambda_i = \lambda_{i\infty} \left(1 + \frac{4h_i}{Re_i \varepsilon}\right)^2 \cong \lambda_{i\infty} \left(1 + \frac{8h_i}{Re_i \varepsilon}\right) \quad (3)$$

where $\lambda_{i\infty}$, Re_i and ε/h_i are the friction factor for turbulent rough flows, the Reynolds number and the relative roughness of the i_{th} layer, respectively. The value of $\varepsilon = 2 \cdot 10^{-5}$ m for both the bottom and sidewalls' roughness was used. $\lambda_{i\infty}$ and Re_i are defined as:

$$\lambda_{i\infty} = \frac{1}{4}\left[\log\left(\frac{3.71\, h_i}{Re_i \varepsilon}\right)\right]^{-2} \quad (4)$$

$$Re_i = \frac{|V_i| h_i}{\nu_i} \quad (5)$$

where ν_i is the kinematic viscosity of the i^{th} layer. Equation (3) shows that the term $8h_i/(\mathrm{Re}_i\, \varepsilon)$ adapts the friction factor for turbulent rough flows to turbulent transition flows. In the performed experiments turbulent transition flows develops.

The shear stress at the interface between the two fluids is defined as:

$$\tau_{12} = \lambda_{12} \frac{\rho_1 + \rho_2}{2} \frac{(V_2 - V_1)|V_2 - V_1|}{8} \quad (6)$$

where λ_{12} is the friction factor at the interface between two different fluids. Adduce et al. (2012) used a constant value λ_{12} = 0.24 for their simulations, while in this study the definition of λ_{12} is improved and expressed as a function of Re_i and given by:

$$\lambda_{12} = \lambda' + \frac{\lambda'' - \lambda'}{1 + e^{-(Re_i - Re_0)}} \quad (7)$$

where $\lambda'' < \lambda'$. All the parameters of relation (7) were calibrated and the following values were obtained: $\lambda' = 0.24$, $\lambda'' = 0.19$, $\mathrm{Re}_0 = 6000$.

In this paper two different entrainment relations were tested: Adduce et al. (2012) relation and Cenedese and Adduce (2010) relation. As discussed in Adduce et al. (2012), Turner (1986) formula, widely used to parametrize mixing, cannot be used to model entrainment for gravity currents produced by a lock exchange, then some modifications to Turner (1986) relation were adopted. Following Adduce et al. (2012) the entrainment parameter is modeled by:

$$E = \frac{V_e}{|V_1 - V_2|} = \frac{k\, Fr_1^2}{Fr_1^2 + 5} \quad (8)$$

where V_e is the entrainment velocity, k is a dimensionless coefficient. The entrainment velocity increases as k increases. The calibration value k=0.95 supplies a correct evaluation of the gravity current's depth and a good simulation of the front's speed of the gravity current. Fr_1 is the Froude number of the gravity current, defined as:

$$Fr_1 = \frac{|V_1|}{\sqrt{h_1 \dfrac{\rho_1 - \rho_2}{\rho_1} g \cos\theta}} \quad (9)$$

The numerical simulations obtained using the entrainment formula (8) are compared to those obtained by Cenedese & Adduce (2010) entrainment formula, given by:

$$E = \frac{V_e}{|V_1 - V_2|} = \frac{Min + A\, Fr_1^{\alpha}}{1 + A \cdot C_{inf}(Fr_1 + Fr_0)^{\alpha}} \quad (10)$$

where:

$$C_{inf} = \frac{1}{Max} + \left(\frac{B}{Re_1^{\beta}}\right) \quad (11)$$

The dimensionless coefficients obtained by Cenedese & Adduce (2010) are: $Min = 4 \cdot 10^{-5}$, $A = 3.4 \cdot 10^{-3}$, $Fr_0 = 0.51$, $\alpha = 7.18$, $Max = 1$, $B = 243.52$ and $\beta = 0.5$. Such parameters are based on both experimental data and oceanic measurements, as discussed in details in Cenedese and Adduce (2010).

The mathematical model was numerically solved by an explicit Mac-Cormack's finite difference scheme with a predictor-corrector scheme, that assures a high scheme's stability by using modest computing resources

Results and discussion

Figure 3 and Figure 4 show the comparison between the images acquired by the camera and numerical profiles at four different time steps after release for Run1 and Run2, respectively. Dashed-dotted lines indicate numerical simulations performed with Equation (10) suggested by Cenedese & Adduce (2010); white lines stand for the simulations carried out by Adduce et al. (2012) relation (with k=0.95); dashed lines are the simulations obtained neglecting the entrainment, i.e. k=0.0 in Equation (8). The effect of mixing is to produce a mass flow from the lighter fluid to the heavier one, causing an increase of the height of the gravity current and therefore a decrease of both the density and velocity of the dense flow. The current's profile simulated with formula (10) is substantially overlapped to the simulated current's profile without entrainment. The entrainment relation suggested in Cenedese and Adduce (2010) provides very low values of the entrainment coefficient ($E \cong Min$) for the range of Froude numbers investigated in the performed experiments (i.e. Fr<1). Therefore, as Figure 3 and Figure 4 show, both the numerical simulations obtained by neglecting the entrainment and the simulations performed with Cenedese & Adduce (2010) formula provide a gravity current thinner if compared with the simulations with the entrainment formula (8).

Figures 5a-d show a comparison between experimental front's position and numerical simulations performed with three different entrainment formulas: Cenedese and Adduce (2010); Adduce et al. (2012), i.e. equation (8); no entrainment. The length scale is the gate position x_0, while the time scale t_0 is defined as:

$$t_0 = \frac{x_0}{\sqrt{g_0' h_0}} \tag{12}$$

Where g_0' is the initial reduced gravity given by:

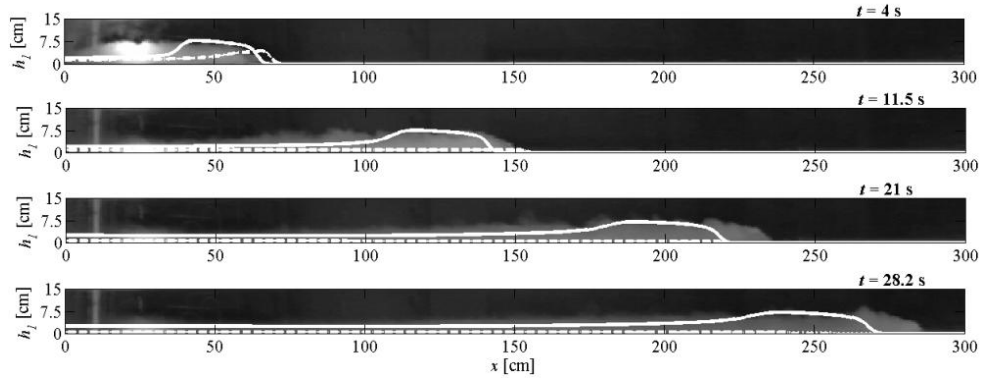

Figure 3: Comparison between the images acquired by the camera at different time steps for Run 1 and numerical simulations with three different entrainment relations: Cenedese and Adduce (2010) (dashed-dotted lines); Adduce et al. (2012) (solid lines); no entrainment (dashed lines).

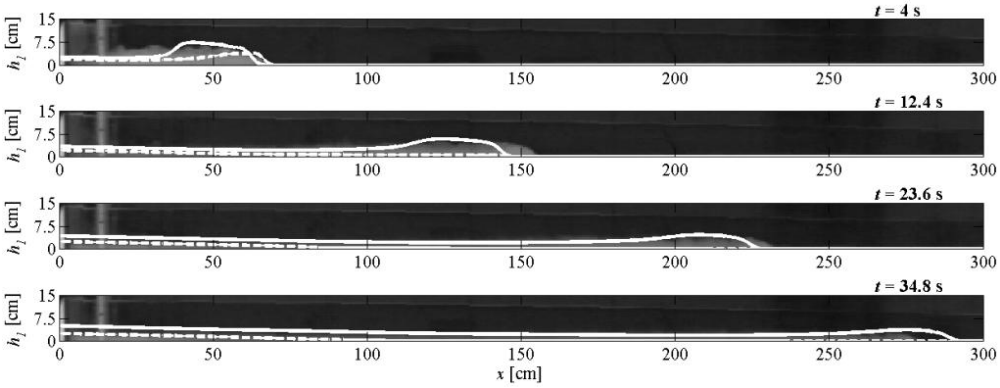

Figure 4: Comparison between the images acquired by the camera at different time steps for Run 2 and numerical simulations with three different entrainment relations: Cenedese and Adduce (2010) (dashed-dotted lines); Adduce et al. (2012) (solid lines); no entrainment (dashed lines).

$$g_0' = g\frac{\rho_{01} - \rho_2}{\rho_2} \quad (13)$$

A good agreement between experimental data and the numerical front's position, predicted with the Adduce et al. (2012) formula, can be observed in Figures 5a-d. For the runs performed on upsloping beds, the simulations without entrainment agree with laboratory data only for a first stage of gravity current's development. The curve obtained by the simulations performed with Cenedese & Adduce (2010) formula is again overlapped to the simulations without entrainment.

In order to define the ability of the model in simulating gravity currents, a Mean Percentage Error (*MPE)* was computed as:

$$MPE = \frac{100}{N}\sum_{j=1}^{N}\left(\frac{\left|x_{nf,j} - x_{ef,j}\right|}{x_{nf,j}}\right) \quad (14)$$

where $x_{nf,j}$ and $x_{ef,j}$ are the numerical and experimental front position, respectively and N is the total number of experimental data. Table 2 shows the evaluated *MPE* for each run. The general trend is that numerical simulations with formula (8) are in better agreement if compared to both the simulations using formula (10) and the simulations without entrainment. When the bed is horizontal, the MPE for the three tested entrainment relations is low. When the bed is upsloping, the MPE for all the simulations with formula (8) is an order of magnitude lower than the MPE of the simulations with both formula (10) and without mixing. Therefore the Adduce et al. (2012) entrainment relation gives good results also for the simulation of gravity currents moving on upsloping beds.

Figures 6a-d show the lower layer velocity, i.e. the velocity of the dense layer, V_1 along x-axis at four different time steps after release for Run 2. The simulated velocity using formula (10), i.e. Cenedese & Adduce (2010), are again overlapped to the simulated velocity without entrainment. Although in Figures 6a-b the three different simulations show a similar general trend for V_1, in a second stage of development (Figures 6c-d), V_1 predicted by formula (8) is different from both the simulations with formula (10) and without entrainment. As it was observed in Figures 5a-d, a low entrainment affects numerical results only after a first stage of the gravity current's development. Furthermore, numerical simulations performed by formula (8), show near the lock an area in which the gravity current's velocity is negative, i.e. the dense fluid is moving downslope. Further laboratory experiments and measurements of instantaneous velocity field will be performed in order to verify the reliability of such a backflow visible in numerical results.

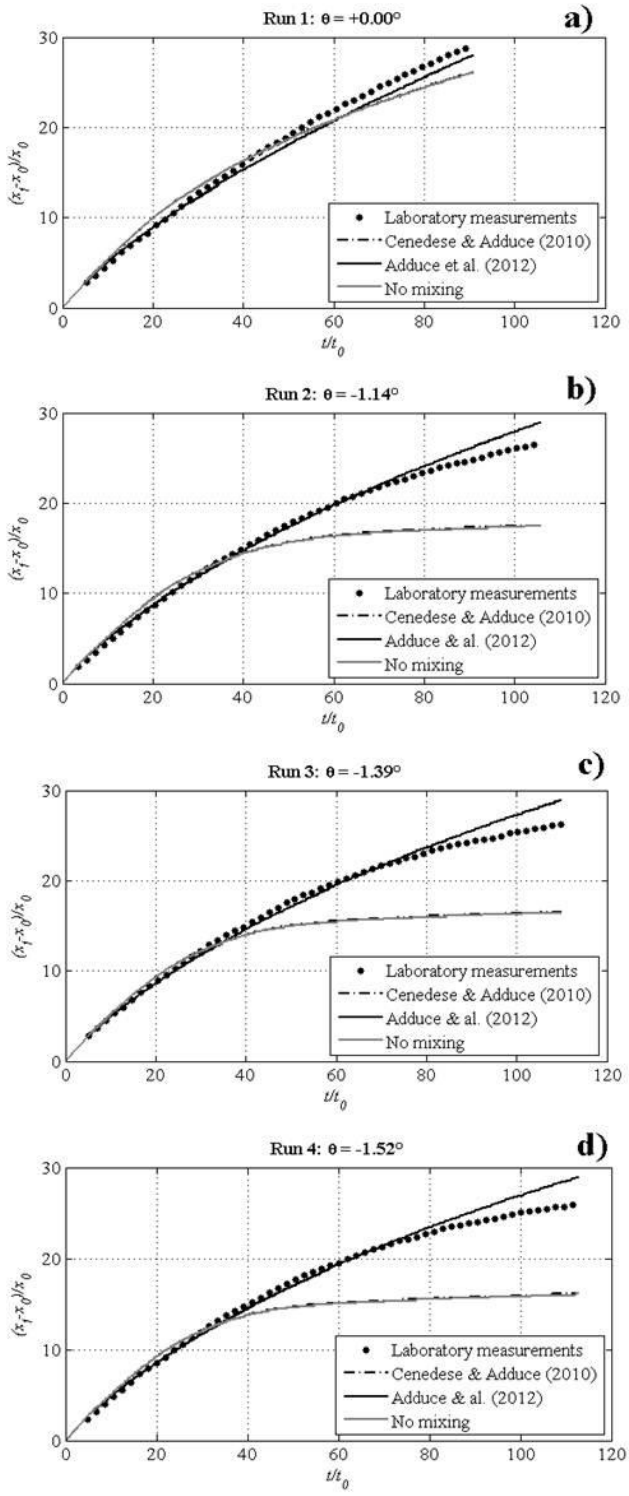

Figure 5a-d: Dimensionless plots of front position versus time for all the performed runs: laboratory measurements (circles), simulations with the Cenedese and Adduce (2010) formula (dash-dotted lines), Adduce et al. (2012) (black lines), no mixing (grey lines).

Table 2: Mean Percentage Error (*MPE*) for each run computed on the basis of Equation (14).

RUN	*MPE* [%]		
	Adduce et al. (2012)	No mixing	Cenedese & Adduce (2010)
1	4.30	6.53	6.43
2	2.91	27.80	27.34
3	3.21	37.34	36.83
4	3.48	37.35	36.84

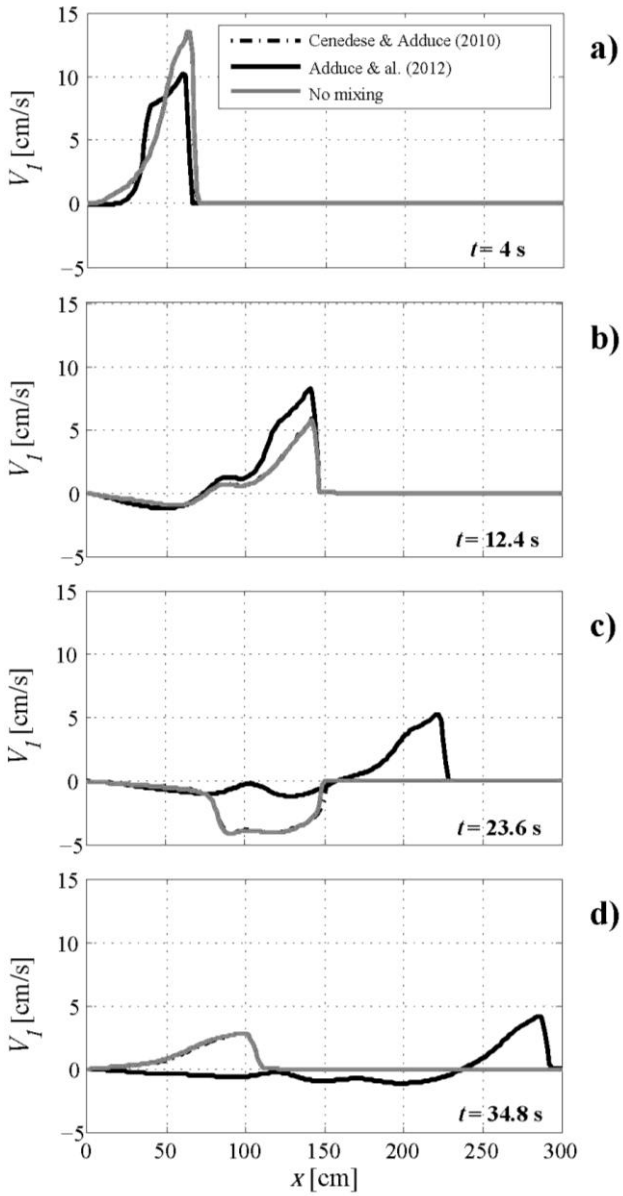

Figure 6a-d: Dense layer velocity V_1 along x-axis, at four different time steps for Run 2, numerical simulations with the formula by: Cenedese and Adduce (2010) (dash-dotted lines); Adduce et al. (2012) (black lines), no mixing (grey lines).

Conclusions

In this work gravity currents moving on both horizontal and upsloping beds are investigated by laboratory experiments and numerical simulations. Experimental gravity currents are realized by full-depth lock exchange release, by changing the bed's slope. All the experiments are recorded by a camera and an image analysis technique is applied to measure the space-time evolution of the gravity currents. Numerical simulations are performed using a two-layer, 1D, shallow-water model, taking into account the free-surface and the mixing occurring at the interface between the two fluids. The entrainment at the interface between the gravity current and the surrounding fluid is modeled by two different formulas: Adduce et al. (2012) entrainment formula, and Cenedese & Adduce (2010) entrainment relation. The comparison between numerical and experimental results shows that the model using Adduce et al. (2012) formula is a valid tool to reproduce the dynamics of lock release gravity currents moving on both horizontal and upsloping beds. The calibration parameter k used in Adduce et al. (2012), for gravity currents moving on horizontal beds, is lower than value of k proposed in the present work. This behavior could be due to the empirical nature of the entrainment relation used, which needs a higher value of k to have good simulations of gravity currents moving on upsloping beds.

References

Adduce, C., Sciortino, G., & Proietti, S. (2012). Gravity currents produced by lock-exchange: experiments and simulations with a two layer shallow-water model with entrainment. *Journal of Hydraulic Engineering*, 138 (2).

Cenedese, C., & Adduce, C. (2010). A new parametrization for entrainment in overflows. *Journal of Physical oceanography* (40), 1835-1850.

Colebrook, C. (1939). Turbulent flows in pipes, with particular reference to the transition region between the smooth and rough pipe laws. *Journal of the Institution of Civil Engineers* (11), 133-156.

Hogg, A., Huppert, H., & Hallworth, M. (1999). Reversing buoynacy of particle-driven gravity currents. *Physics of Fluids* (11), 2891-2900.

La Rocca, M., Adduce, C., Sciortino, G., & Bateman Pinzon, A. (2008). Experimental and numerical simulation of three-dimensional gravity currents on smooth and rough bottom. *Physics of Fluids*, 106603.

Rottmann, J., & Simpson, J. (1983). Gravity currents produced by instantaneous releases of a heavy fluid in a rectangular channel. *Journal of fluid Mechanics* (135), 95-110.

Shin, J., Dalziel, S., & Linden, P. (2004). Gravity currents produced by lock exchange. *Journal of Fluid Mechanics, 521*, 1-34.

Simpson, J. (1997). *Gravity currents in the environment and laboratory.* Cambridge: Cambridge University Press.

Sparks, R., Bonnecaze, R., Huppert, H., Lister, J., Hallworth, M., Mader, H., & Phillips, J. (1993). Sediment-laden gravity currents with reversing buoyancy. *Earth and Planetary Science Letters* (114), 243-257.

Turner, J. S. (1986). Turbulent entrainment: the development of the entrainment assumption, and its application to geophysical flows. *J. Fluid Mech*., 173, 431-471